

Fabrication of 7.2% Efficient CZTSSe Solar Cells Using CZTS Nanocrystals

Qijie Guo,[†] Grayson M. Ford,[†] Wei-Chang Yang,[‡] Bryce C. Walker,[†] Eric A. Stach,[‡]
Hugh W. Hillhouse,^{*,§} and Rakesh Agrawal^{*,†}

School of Chemical Engineering and the Energy Center, Purdue University, West Lafayette, Indiana 47906, United States, and School of Materials Engineering and Birck Nanotechnology Center, Purdue University, West Lafayette, Indiana 47906, United States

Received September 23, 2010; E-mail: h2@uw.edu; agrawalr@purdue.edu

Abstract: Earth abundant copper-zinc-tin-chalcogenide (CZTSSe) is an important class of material for the development of low cost and sustainable thin film solar cells. The fabrication of CZTSSe solar cells by selenization of CZTS nanocrystals is presented. By tuning the composition of the CZTS nanocrystals and developing a robust film coating method, a total area efficiency as high as 7.2% under AM 1.5 illumination and light soaking has been achieved.

Earth abundant copper-zinc-tin-chalcogenide (herein collectively denoted as CZTSSe) thin films have attracted increasing attention for photovoltaic applications. Various vacuum and nonvacuum based thin film deposition techniques have been reported for the preparation of CZTSSe thin films.^{1–7} Of particular interest are solution based thin film deposition methods, as they promise to lower manufacturing costs and yield higher throughput.^{3,5,8} Recently, Todorov et al. reported the fabrication of CZTSSe thin film solar cells with 9.6% power conversion efficiency (PCE) using a hydrazine-based solution via spin coating.⁸ These exciting results demonstrate the promise of CZTSSe for low-cost solar cells. However, hydrazine is a highly toxic and very unstable compound that requires extreme caution during handling and storage. As a result, it is desirable to develop a robust, easily scalable, and relatively safe solution-based process for the fabrication of device quality CZTSSe thin films and resulting high efficiency solar cells.

Previously, we have demonstrated the fabrication of various multinary chalcogenide thin films and solar cells, including CuInSe₂, Cu(In,Ga)(S,Se)₂, and CuZnSn(S,Se)₂, by sintering the corresponding chalcogenide nanocrystals in the presence of selenium vapor.^{3,9,10} Preliminary results from solar cells fabricated using CZTS nanocrystals indicated this approach is potentially viable, even though the efficiencies were less than 1%. Here, we have addressed some of the efficiency-limiting challenges and problems encountered in our previously reported devices. Significant improvements in the PCE have been achieved by tuning the composition of the as-synthesized CZTS nanocrystals and by developing a robust thin film coating method. Moreover, the as-fabricated CZTSSe solar cells showed exceptional stability under standard laboratory conditions, with a slight improvement in device performance observed after a three-month period. A total area (0.47 cm², including the shaded areas by the evaporated Ni/Al contacts) PCE of 7.2% has been achieved under AM 1.5 illumination after light soaking for 15 min.

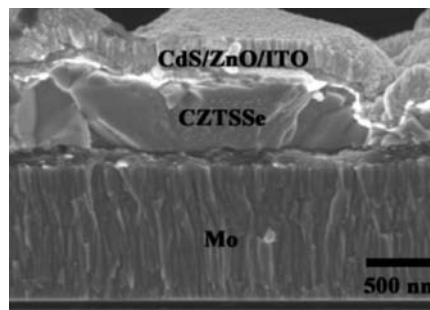


Figure 1. Cross section FE-SEM image of a completed CZTSSe thin film solar cell. The selenized CZTSSe film exhibits large densely packed grains, desired for high efficiency devices.

CZTS nanocrystals are synthesized by hot injection, as detailed in a previous report,³ with slight changes in the amounts of the cation precursors. The overall composition of the nanocrystals is kept copper poor in accordance with copper poor and zinc rich compositions widely adapted in the literature.^{4,8} Excess copper has been shown to result in the formation of binary and/or ternary phases of copper chalcogenide in the final film, resulting in poorer device performance. Thus, the amounts of the Cu, Zn, and Sn precursors used in a typical synthesis are 1.332 mmol, 0.915 mmol, and 0.75 mmol respectively. Oleylamine (Technical grade, Aldrich) is used as the sole solvent, as previously described. After the reaction mixture is purged, the temperature is raised to 225 °C where 4 mL of 1 M sulfur-oleylamine are injected and the temperature is held for 30 min. After the reaction, CZTS nanocrystals are collected by centrifugation using equal amounts of hexane and ethanol. Residual oleylamine is then removed by repeated washing using hexane/isopropanol (1:2 ratio) using a centrifuge (10 000 rpm for 5 min). The final precipitate is then dried under a stream of argon and redispersed in hexanethiol (Aldrich) to form a stable ink with a concentration of ~200 mg/mL. The composition of the as-synthesized copper poor CZTS nanocrystals is Cu_{1.31±0.02}Zn_{0.91±0.03}Sn_{0.95±0.02}S₄, as determined by averaging over 10 random spots using energy dispersive X-ray spectroscopy (EDS - FEI Quanta). The size and shape of the as-synthesized copper poor CZTS nanocrystals are similar to those of the stoichiometric nanocrystals synthesized previously.⁶ Also, no noticeable impurity phases were observed using powder X-ray diffraction (PXRD). However, it is important to acknowledge that PXRD alone is insufficient to determine the phase purity of the CZTS nanocrystals, since many of the binary and ternary chalcogenides share similar crystal structures.¹¹ Therefore, supplementary techniques including Raman spectroscopy, photoluminescence, electron diffraction, and composition mapping using HR-TEM are currently underway to determine the phase purity of the as-synthesized CZTS nanocrystals: these will be reported in a follow-up study.

The hexanethiol dispersed CZTS nanocrystals can be applied directly onto molybdenum (~1 μm) coated soda lime glass

[†] School of Chemical Engineering and the Energy Center.

[‡] School of Materials Engineering and Birck Nanotechnology Center.

[§] Current Address: Department of Chemical Engineering, University of Washington, Seattle, WA 98195.

substrates by knife coating to form a densely packed nanocrystal thin film. A layer of scotch tape is typically used as the spacer for knife coating. Two coatings of the CZTS nanocrystals are applied for a total film thickness of approximately $1\ \mu\text{m}$. After each coating, the films are dried on a hot plate in air at $300\ ^\circ\text{C}$ for 1 min. The CZTS nanocrystal films are then subjected to annealing at $500\ ^\circ\text{C}$ for 20 min under Se vapor in a graphite box (hereafter "selenization") to replace the majority of the sulfur with selenium and enhance grain growth. After selenization, the resulting CZTSSe film is composed of large densely packed grains (Figure 1), an important morphological feature for high efficiency thin film solar cells. The final films have a Cu/(Zn + Sn) ratio of 0.79 and a Zn/Sn ratio of 1.11, consistent with other high efficiency CZTS devices and indicating Sn loss during selenization. The sintered CZTSSe absorber films are processed into photovoltaic devices following standard procedures, including chemical bath deposition of CdS ($\sim 50\ \text{nm}$), RF sputtering of *i*-ZnO ($\sim 50\ \text{nm}$), RF sputtering of ITO ($\sim 200\ \text{nm}$), and thermal evaporation of a patterned Ni/Al grid as the top contact. Finally, the samples are mechanically scribed into individual cells with a total area of $0.47\ \text{cm}^2$. Figure 1 shows a representative cross section field-emission scanning electron microscope (FE-SEM) image of a completed CZTSSe solar cell.

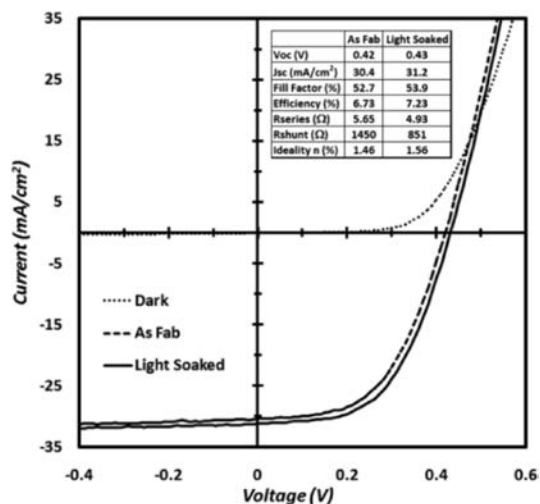


Figure 2. *I*–*V* characteristics of the best performing CZTSSe solar cell measured in the dark, as fabricated, and after light soaking for 15 min under AM 1.5 illumination. The reported device parameters are calculated based on total device area ($0.47\ \text{cm}^2$).

The current–voltage (*I*–*V*) characteristics for the best performing CZTSSe solar cell measured in the dark, under AM 1.5 illumination, and after light soaking for 15 min under one sun illumination are shown in Figure 2. All device performance parameters are reported based on total cell area, including the shaded areas ($\sim 5\%$ of total device area) shaded by the Ni/Al fingers. The as-fabricated device shows a total area efficiency of 6.7% ($V_{\text{oc}} = 0.42\ \text{V}$, $J_{\text{sc}} = 30.4\ \text{mA}/\text{cm}^2$, $\text{FF} = 52.7\%$). The overall PCE is limited by a high series resistance ($5.6\ \Omega$), resulting in a substantial loss in fill factor. It is expected that a significant improvement in device performance can be achieved by improving the sheet resistances of the Mo and ITO layers (currently at ~ 5 and $\sim 80\ \Omega/\square$, respectively). Interestingly, the CZTSSe solar cells also show serendipitous stability over time, similar to that commonly observed for CIGSSe based solar cells.¹² The photon conversion efficiency of the device improved to 6.89% after sitting in standard laboratory conditions for three months (data not shown). The efficiency is further improved to 7.2% after light soaking for 15 min under one sun illumination. However, the change

in device performance is temporary and PCE goes back down to its starting point after the light is turned off.

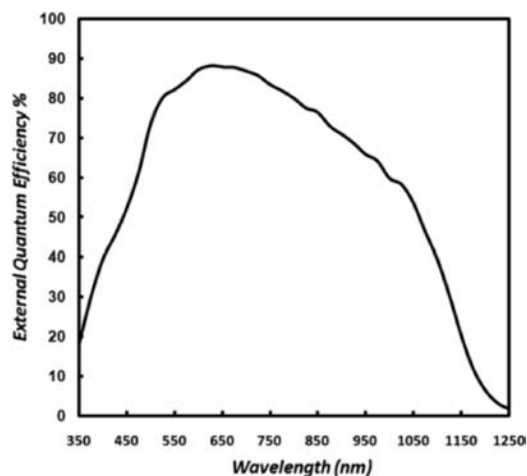


Figure 3. External quantum efficiency (EQE) of the corresponding best performing CZTSSe solar cell. The band gap of the absorber is approximated to be $\sim 1.05\ \text{eV}$ by extrapolation.

Figure 3 shows the external quantum efficiency (EQE) of the corresponding CZTSSe solar cell. The quantum efficiency in the visible range is promising ($\sim 90\%$); however it drops off significantly in the near-IR range. The loss of quantum efficiency in longer wavelengths is due to a nonoptimal thickness of the CZTSSe absorber layer in the current devices. Typical absorption coefficients reported for CZTSSe thin films are in the range of 10^4 – $10^5\ \text{cm}^{-1}$, which suggests that a thicker absorber is needed to effectively absorb the solar spectrum and reduce recombination at the back contact.^{13,14} The highest efficiency CZTSSe solar cell reported by Todorov et al. had an absorber thickness $>2.5\ \mu\text{m}$.⁸ As a result, significant improvement for longer wavelengths may be obtained with thicker absorber layers provided minority carrier lifetimes are sufficiently long. Initial experiments with thicker absorber layers have shown lower efficiencies due to increased series resistance, suggesting the fabrication process must be optimized for thicker films. The band gap of the final CZTSSe absorber estimated from the EQE data is $\sim 1.05\ \text{eV}$, which is significantly lower than that reported for all sulfur variant CZTS ($\sim 1.5\ \text{eV}$).^{13,14} The change in band gap energy is due to the replacement of S by Se (analogous to the case of CIGS/CIGSe), which can be exploited for fine-tuning the band gap of CZTSSe for improved performance.

In conclusion, a robust, solution-based method for the fabrication of efficient CZTSSe thin film solar cells has been reported. A total area power conversion efficiency of 7.2% has been achieved after light soaking. The overall device fabrication techniques are readily scalable and can be easily adapted to flexible or rigid substrates.

Acknowledgment. Q.G. would like to thank the Purdue Research Foundation Trask Fund, G.M.F. would like to thank the Conoco Philips Fellowship, and W.Y. and B.C.W. would like to thank the NSF Solar Economy IGERT program for financial support.

References

- (1) Tanaka, T.; Kawasaki, D.; Nishio, M.; Gu, Q. X.; Ogawal, H. *Phys. Status Solidi C* **2006**, *3* (8), 2844–2847.
- (2) Ennaoui, A.; Lux-Steiner, M.; Weber, A.; Abou-Ras, D.; Kotschau, I.; Schock, H. W.; Schurr, R.; Holzinger, A.; Jost, S.; Hock, R.; Voss, T.; Schulze, J.; Kirbs, A. *Thin Solid Films* **2009**, *517*, 2511–2514.
- (3) Guo, Q.; Hillhouse, H. W.; Agrawal, R. *J. Am. Chem. Soc.* **2009**, *131*, 11672–11673.
- (4) Katagiri, H.; Jimbo, K.; Maw, W. S.; Oishi, K.; Yamazaki, M.; Araki, H.; Takeuchi, A. *Thin Solid Films* **2009**, *517*, 2455–2460.

- (5) Steinhagen, C.; Panthani, M. G.; Akhavan, V.; Goodfellow, B.; Koo, B.; Korgel, B. A. *J. Am. Chem. Soc.* **2009**, *131*, 12554–12555.
- (6) Tanaka, K.; Oonuki, M.; Moritake, N.; Uchiki, H. *Sol. Energy Mater. Sol. Cells* **2009**, *93*, 583–587.
- (7) Wadia, C.; Alivisatos, A. P.; Kammen, D. M. *Environ. Sci. Technol.* **2009**, *43*, 2072–2077.
- (8) Todorov, T. K.; Reuter, K. B.; Mitzi, D. B. *Adv. Mater.* **2010**, *22*, E156–E159.
- (9) Guo, Q.; Kim, S. J.; Kar, M.; Shafarman, W. N.; Birkmire, R. W.; Stach, E. A.; Agrawal, R.; Hillhouse, H. W. *Nano Lett.* **2008**, *8*, 2982–2987.
- (10) Guo, Q.; Ford, G. M.; Hillhouse, H. W.; Agrawal, R. *Nano Lett.* **2009**, *9*, 3060–3065.
- (11) Fernandes, P. A.; Salome, P. M. P.; da Cunha, A. F. *Thin Solid Films* **2009**, *517*, 2519–2523.
- (12) Guillemoles, J.; Rau, U.; Kronik, L.; Schock, H.; Cahen, D. *Adv. Mater.* **1999**, *11*, 957.
- (13) Ito, K.; Nakazawa, T. *Jpn. J. Appl. Phys., Part 1* **1988**, *27*, 2094–2097.
- (14) Seol, J. S.; Lee, S. Y.; Lee, J. C.; Nam, H. D.; Kim, K. H. *Sol. Energy Mater. Sol. Cells* **2003**, *75*, 155–162.

JA108427B